

Tc interaction with crystalline rock from Äspö (Sweden): Effect of in-situ rock redox capacity

Florian Mathias Huber ^{a,*}, Yury Totstkiy ^a, Rémi Marsac ^a, Dieter Schild ^a, Ivan Pidchenko ^a, Tonya Vitova ^a, Stepan Kalmykov ^b, Horst Geckeis ^a, Thorsten Schäfer ^a

^a Karlsruhe Institute of Technology (KIT), Institute for Nuclear Waste Disposal (INE), P.O. Box 3640, D-76021 Karlsruhe, Germany

^b Lomonosov Moscow State University (MSU), Department of Chemistry, Leninskie Gory 1-3, 119991, Moscow, Russia

A B S T R A C T

The interaction of Tc(VII) with crushed crystalline rock (Äspö diorite; 1–2 mm size fraction) from the Äspö Hard Rock Laboratory (HRL) (Sweden) was studied by laboratory batch sorption and desorption experiments under Ar atmosphere using both natural and synthetic groundwater. The Äspö diorite used in the experiments was drilled, transported and handled as far as possible under anoxic conditions to preserve the in situ rock redox capacity. For comparison, identical experiments using artificially oxidized Äspö diorite have been carried out to examine the effect of in situ redox capacity on Tc uptake. According to the batch studies, Tc(VII) uptake on the Äspö diorite is strongly dependent on redox capacity. Uptake on an oxidized rock is approximately 2 times higher compared to unoxidized rock samples, most likely due to higher Fe(II) contents of the unoxidized rock. Tc redox states and speciation both on the mineral surface and in the bulk were studied using X-ray photoelectron spectroscopy (XPS) and Tc K edge X-ray absorption near edge structure (XANES) spectroscopy. The spectroscopic results verify a Tc(VII) reduction to Tc(IV) at the rock surface. Distribution coefficients (K_d) and surface normalized distribution coefficients (K_a) were determined and compared to available literature data. The formation of a Tc colloidal phase was not observed under the geochemical conditions prevailing in the experimental studies. Desorption of Tc is very low under anoxic conditions, but after artificial oxidation Tc mobility is strongly increased. The results of this work clearly highlight the effect of in situ rock redox capacity on Tc retention.

1. Introduction

The generally accepted concept of spent nuclear fuel (SNF) and high level nuclear waste (HLW) long term storage is by disposal in deep geological formations at depths of around 250–1000 m (IAEA, 2001). The repository host rock as part of a multi barrier system plays an important role as retention barrier for radionuclide migration. Thus, the selection of the host rock formation with appropriate geochemical and hydrogeological properties is a key challenge during nuclear waste repository siting and it requires comprehensive scientific research. Crystalline rocks (e.g. granites and gneisses) are considered as potential host rock formations for

* Corresponding author. Karlsruhe Institute of Technology (KIT), Institute for Nuclear Waste Disposal (INE), Hermann-von-Helmholtz-Platz 1, 76344 Eggenstein-Leopoldshafen, Germany.

E-mail address: florian.huber@kit.edu (F.M. Huber).

the deep geological disposal in several countries (e.g. Sweden, Finland, Russia, Korea). The work described herein focuses on crystalline rock samples from the Äspö Hard Rock Laboratory (HRL) (Sweden) which is a generic underground research laboratory (URL) located on the Äspö island near Oskarshamn in southern Sweden dedicated to in situ studies of processes in crystalline formations concerning deep geological disposal of spent nuclear fuel (SKB, 2011). Radionuclide transport depends strongly on the bedrock hydrogeological and geochemical conditions (pH, Eh, and ionic strength) and is governed by different immobilization/remobilization processes (Grambow, 2008). The most important retention processes to be considered in fractured crystalline rocks are sorption to rock surfaces, redox reactions and matrix diffusion (Bodin et al., 2003; Neretnieks, 1980; Xu and Worman, 1999).

⁹⁹Tc is one of the main long lived U and Pu fission products in SNF and is also generated by medical laboratories and research institutions. Because of its relatively high fission yield (ca. 6%) and

long half life (2.1×10^5 years) ^{99}Tc is considered as a radioactive component of HLW with significant toxic relevance (Kratz and Lieser, 2013). Technetium mobility in natural systems strongly depends on the redox state. The most stable Tc form under aerobic atmosphere is the pertechnetate ion TcO_4^- , which is very soluble and behaves like a conservative tracer under oxidizing conditions (Rard et al., 1999). In an early work by Bondietti and Francis (1979) using a variety of natural rock materials considerable Tc retention due to reduction of pertechnetate was observed in accordance with Eh/pH conditions. The potential of the $\text{TcO}_4^-/\text{TcO}_2$ couple was described with equation (1) (Meyer and Arnold, 1991):

$$E_0\left(\text{TcO}_4^-/\text{TcO}_2\right) = 0.738 - 0.0788 \times \text{pH} + 0.0197 \times \log\left[\text{TcO}_4^-\right] \quad (1)$$

Under aerobic conditions, reported K_d values of Tc on crystalline rocks are negligible, < 1 mL/g in Allard et al. (1979) (contact time 1 day) and < 0.1 – 8.6 mL/g in Videnska and Havlova (2012) (contact time with granitic rocks up to 94 days), whereas under reducing conditions the values are much higher (50 mL/g in Allard et al. (1979)). Both batch type sorption and column experiments with Hanford sediments (Um and Serne, 2005; Zachara et al., 2007) have revealed that ^{99}Tc is highly mobile and shows virtually no retardation under fully oxidizing conditions. However, under anoxic conditions TcO_4^- is prone to reduction to Tc(IV) and the solubility is limited by the hydrous oxide solid phase $\text{TcO}_2 \cdot 1.6\text{H}_2\text{O}_{(s)}$ (Meyer et al., 1991). As a consequence, distribution coefficients and apparent diffusion coefficients of technetium reported in the literature on natural minerals are scarce and are rarely published together with the respective pe and pH conditions. Tc redox kinetics strongly depend on the availability of reactive Fe(II) in the host rock and the mineral association and speciation on surface (surface complexed, precipitated, and ion exchangeable) (Fredrickson et al., 2009; Heald et al., 2007; Jaisi et al., 2009; Peretyazhko et al., 2008a, 2008b; Zachara et al., 2007). Aspo *in situ* and laboratory migration studies (CHEMLAB 2) using Aspo derived natural groundwater revealed $\approx 1\%$ Tc recovery (after 254 days) of the injected Tc(VII) mass (Kienzler et al., 2003, 2009). Batch type studies done in parallel revealed surface normalized distribution coefficients, K_a , values of $\approx 2.1 \times 10^{-3}$ m for ^{99}Tc ($t_{\text{contact}} = 14$ d), whereas altered material showed significantly lower values. These results revealed contact/residence time dependent retardation and/or reduction processes. In all studies mentioned above, though carried out under e.g. Ar atmosphere in glove boxes, crystalline rock materials used were exposed for a considerable time to air before the experiments. This circumstance might be one of the most important drawbacks in all batch sorption/desorption studies carried out not only on redox sensitive radionuclides but for redox sensitive heavy metals in general. Due to the drastically increased effort in preserving the natural *in situ* rock redox capacity during drilling, transporting and storing of the rock material, almost no studies are available using non oxidized material. In consequence, the distribution coefficients, sorption and reduction properties and behaviour published in numerous studies could be biased and accompanied with high uncertainties. So far, only one study on U interaction with the same un oxidized Aspo diorite (AD) material (provided by KIT INE) as used in the present study is available (Schmeide et al., 2014). Therefore, the main motivation of this work is to investigate the effect of *in situ* rock redox capacity on technetium sorption behaviour by conducting classical batch experiments using non oxidized and oxidized rock material, respectively.

2. Materials and methods

2.1. Radionuclides

2.1.1. ^{99}Tc

All Tc batch experiments with Tc concentration $\geq 10^{-9}$ M have been carried out using a ^{99}Tc stock solution (13 mM NaTcO_4) produced at the former Institute of Hot Chemistry, Nuclear Research Centre (former FZK, now KIT) (Karlsruhe, Germany). The solubility limit of Tc(IV) in a wide range of pH Eh conditions covering most of the natural systems is about 4.4×10^{-9} M (Duro et al., 2006). The detection limit of low background liquid scintillation counting (LSC) (Quantulus, PerkinElmer, Inc., LSC cocktail Ultima Gold) for ^{99}Tc measurement is $\approx 10^{-10}$ M.

2.1.2. ^{95m}Tc

For experiments with Tc concentrations lower than 10^{-9} M, ^{95m}Tc with a much shorter half life (61 day) and a main gamma emission line at 204.1 keV was applied. The isotope was produced by proton irradiation of natural Mo foil (50 μm thickness) containing the natural isotopic composition at ZAG Zyklotron AG (Karlsruhe, Germany). After cooling the foil was transported to the Institute for Nuclear Waste Disposal (KIT INE) and processed to separate technetium according to the technique of Boyd et al. (1960). The foil was dissolved in a mixture of concentrated H_2SO_4 and 30% H_2O_2 and afterwards slowly neutralized with saturated NaOH (up to alkaline pH). The obtained alkaline solution was passed through a column filled with the anion exchanger Dowex 1 \times 8 (100–200 mesh particle size) with a total volume of ca. 3 mL. The column was washed first with 20 mL 1 M $\text{K}_2\text{C}_2\text{O}_4$ to remove residues of molybdate and after rinsing with 20 mL of MilliQ water pertechnetate was eluted with 30 mL 1 M HClO_4 . The last fraction was collected into 2 mL vials, which were measured with γ spectrometry and samples with ca. 90% of ^{95m}Tc were combined and neutralized with concentrated NaOH. The purification level was monitored with ICP MS and γ spectrometry. The use of another column filled with Teva[®] Resin (Eichrom Technologies, LLC) prior to Dowex significantly increased chemical purity of Tc. Technetium separation on Teva Resin column was performed from ≈ 1.5 M HNO_3 media and after washing the column with 2 M HNO_3 Tc was eluted with 8 M HNO_3 according to the technique reported by Tagami and Uchida (1999). A further separation step on the Dowex column results in the purification from NO_3^- , which may act as undesired oxidizing agent, being absent in natural deep geological anoxic groundwaters. The nitrate concentration was initially controlled with nitrate test strips (Merck) and subsequent ion chromatography (IC) analysis. Detection limit of gamma spectrometric analysis of ^{95m}Tc using a 10 mL vial geometry and a high purity germanium (HPGe) semiconductor detector was estimated to be $\approx 10^{-14}$ – 10^{-15} M (three hours measurement time) depending on the age of the stock solution.

2.2. Solid materials

2.2.1. Aspo diorite

Diorite is the dominating rock type in the Aspo area (Kornfalt et al., 1997). The general mineralogical characterization of AD is presented in Table 1. Fresh Aspo diorite was obtained from a drilling campaign at the Aspo HRL (Sweden) in 2011 within the EU project CP CROCK. Details of the sampling procedure and material characterization were originally published within a CROCK S&T contribution (Schafer et al., 2012). During the core drilling, special care was taken to minimize the exposure of the solid material to air. Therefore, the drilling procedure was carried out with a double tube technique preserving to the best possible anoxic conditions.

Table 1

Petrographic characterization of Aspo diorite (Byegård et al., 1998; Kornfalt et al., 1997).

Material	Rock type	Mineralogical composition, %	Structural characteristic
Aspo diorite	Quartz monzodiorite/granodiorite	Plagioclase, 30-50 Quartz, 10-25 K-feldspar, 10-30 Biotite, 10-25 Epidote, 3-15 Amphibole (mainly hornblende), <10 Muscovite, titanite, apatite, fluorite, zircon, magnetite	Porphyritic, medium-grained

Natural Aspo groundwater ($E_{\text{SHE}} \approx 240$ mV) permanently bubbled with N_2 was used as a drilling fluid. After a short visual inspection (max. 5 min) under tunnel atmosphere the cores were directly transferred into a transparent LD PE bag, which was evacuated three times (≈ 0.4 bar) and purged with nitrogen gas before welding. The same procedure was applied with an Al bag for the second confinement to prevent oxidation during transportation to the KIT INE laboratories (see Figure A1, bottom). At KIT INE the cores were stored in a barrel under Ar atmosphere (≈ 1 bar over pressure). Two Aspo diorite drill cores (borehole KA2368A 01, cores #1.32 and #1.33) were selected for the experiments. Both cores were chosen because of their (maximal) distance to the tunnel wall (13.04–13.52 m (core #1.32) and 13.52–14.00 m (core #1.33)) and their petrological characterization (fresh Aspo diorite) during the drilling campaign (Figure A1, top and middle). For preparation of the crushed material, the cores were transferred into an Ar glovebox equipped with a circular diamond saw and cut into small discs (0.5–1 cm in width). These discs were then manually crushed with a hammer and separated into several size fractions by sieving. For the sorption experiments the 1–2 mm size fraction in diameter was chosen. A N_2 BET specific surface area of $0.16 \text{ m}^2/\text{g}$ was measured for this size fraction. This un oxidized crushed material was stored permanently in the glovebox under Ar atmosphere (≤ 1 ppm O_2). Part of this crushed diorite material was exposed to air for one week for artificial surface oxidation to investigate the influence of sample preservation and preparation on Tc uptake. The chemical composition of the rock material used was determined at the Institute for Geosciences, Johannes Gutenberg University (Mainz, Germany) by X Ray fluorescence (XRF) spectrometry (spectrometer MagiXPRO, Philips) with a Rh anode operated at 3.2 kW). In Table A1 the XRF data for the material studied is compared to the oxidized Aspo diorite used by Huber et al. (2012, 2010) and to material from Byegård et al. (1998). A typical granodiorite composition (Nockolds, 1954) is also added in Table A1 for comparison. The general composition of the AD is typical of granitic rocks with high amount of SiO_2 and Al_2O_3 (quartz and feldspar) (Nockolds, 1954). The Fe^{2+} content of the solid phases was measured by cerimetric titration (cerate oximetry) with potentiometric end point determination (Close et al., 1966). The new un oxidized AD shows a much higher amount of ferrous iron ($\approx 39\% \text{ Fe}^{2+}/\text{Fe}_{\text{tot}}$ vs. $\approx 27\%$ in old AD samples) compared to the old oxidized AD. This result gives confidence in the approach carried out to preserve the in situ rock redox capacity. In the work by Byegård et al. (1998) no information on Fe(II) compounds were reported. In order to estimate the cation exchangeable Fe(II) amount on the mineral surfaces of the Aspo diorite, a method proposed by Heron et al. (1994) was applied using 10 mL 1 M CaCl_2 (pH 7) in contact with 2 g of granite for 24 h. Afterwards, an aliquot was taken for Fe(II) quantification by the ferrozine technique. The analytical procedure of the ferrozine technique is described in Viollier et al. (2000). Additionally, Fe data on the new un oxidized and old oxidized AD material determined by cerimetric titration are given in Table A1 showing that the overall Fe(II)

redox buffer is drastically reduced for the oxidized samples. The ion exchangeable Fe(II) fraction for the un oxidized AD was quantified at approx. 4–6 $\mu\text{g}/\text{g}$, whereas for the oxidized samples lower values around 1–3 $\mu\text{g}/\text{g}$ for AD are obtained. The rather high uncertainty in the measurements is attributed to the natural heterogeneity of the rock material. The content of ion exchangeable Fe(II) is about three orders of magnitude lower than Fe(II) amount in the bulk obtained by cerimetric titration (see Table A1). However, the ratio between Fe(II) content in fresh and oxidized materials of the order of three is similar for both types of measurements.

2.3. Groundwater

Different types of groundwater have been used in the experimental program. Besides the natural Aspo groundwater (AGW) a synthetic groundwater simulant (AGWS) has been prepared to mimic the CROCK drilling site outflow groundwater composition (see Schafer et al. (2012)). All chemicals used in the preparation of the synthetic groundwater were of analytical grade. Solutions were prepared with deionized Milli Q water which was stripped with Ar prior to use. AGWS has a comparable composition to natural Aspo groundwater sampled *in situ* from borehole KA3600 F 2 stored in a Ar pre flushed 50 L Teflon coated Al barrel at the CP CROCK site (Heck and Schafer, 2012). Chemical compositions of the AGWS used and natural groundwater samples from Aspo and Grimsel (GGW) (glacial melting water analogue with low ionic strength) are presented in Table 2. Relatively high Eh values of AGWS and GGW is explained by the low concentration of the redox couples (e.g. Fe(II)/Fe(III)) in the solution which cannot be measured using a Pt electrode.

2.4. Batch experiments

2.4.1. Sorption experiments

Before the start of the batch sorption kinetic experiments the crushed material was contacted with relevant groundwater simulant (GWS) for one day and exchanging the water five times. This step was conducted to remove any remaining fines/colloids from the sieving procedure. In case of un oxidized AD the last step was performed with natural AGW to establish more realistic conditions. All batch experiments were carried out in 20 mL LSC vials (HDPE, Zinsser®) inside an Ar glovebox with O_2 concentrations ≤ 1 ppm at room temperature (20 ± 2 °C). The solid to liquid ratio chosen was 2.0 g of granitic rock and 8.0 mL of groundwater (250 g/L). Sample duplicates were prepared and kept closed during the sorption experiments to prevent oxidation of Fe(II) at the mineral surfaces. All sorption experiments were conducted at pH 8.1 ± 0.05 . Tc(VII) concentrations of 1×10^{-5} M, 1×10^{-8} M, and 1×10^{-9} M were used in the experiments. For measurement of ^{99}Tc content in the sample supernatant after the desired contact time, 1 mL aliquots were taken and added to 10 mL of Ultima Gold LSC cocktail for analysis with LSC. To differentiate between potentially formed

Table 2

Overview of the chemical compositions of the synthetic Aspo groundwater simulant (AGWS), Aspo groundwater and Grimsel groundwater, respectively. Eh_(SHE) denotes corrected Eh.

	AGWS	AGWS after 122 h contact time	Aspo GW (KA-3600-F-2)	Grimsel GW (MI-shear zone)
pH	8.0 ± 0.05	8.0 ± 0.05	7.8 ± 0.05	9.67 ± 0.05
Eh _(SHE)	390 ± 50 mV	n.m.	-240 ± 50 mV	320 ± 50 mV
[Mg]	104 ± 1.0 mg/L	104.6 mg/L	69.4 mg/L	12.6 µg/L
[Ca]	1109 ± 94 mg/L	1134 mg/L	1135 mg/L	5.3 µg/L
[K]	19.35 ± 3.86 mg/L	21.56 mg/L	10.5 mg/L	
[Li]	2.53 ± 0.04 mg/L	2.50 mg/L	6.0 mg/L	
[Fe]	n.m.	n.m.	0.2 mg/L	< D.L.
[Mn]	2.32 ± 3.02 µg/L	23.8 µg/L	0.338 mg/L	< D.L.
[Sr]	19.68 ± 0.29 mg/L	20.14 mg/L	19.9 mg/L	182 µg/L
[Cs]	<D.L.	< D.L.		0.79 µg/L
[La]	n.m.	n.m.		< D.L.
[U]	0.05 ± 0.01 µg/L	1.70 µg/L	0.11 µg/L	0.03 µg/L
[Th]	0.02 ± 0.01 µg/L	0.07 µg/L	<0.01 µg/L	<0.01 µg/L
[Al]	182.8 ± 56.3 µg/L	439.6 µg/L	13.3 µg/L	42.9 µg/L
[Na]	1929 ± 29 mg/L	1905 mg/L	1894 mg/L	14.7 mg/L
[Cl]	4749 ± 145 mg/L	4895 mg/L	4999 mg/L	6.7 mg/L
[Si]	n.m.	n.m.	4.7 mg/L	5.6 mg/L
[SO ₄]	409 ± 5.0 mg/L	411.88 mg/L	394.4 mg/L	5.8 mg/L
[F]	1.97 ± 0.09 mg/L	1.98 mg/L	1.41 mg/L	6.3 mg/L
[Br]	21.17 ± 0.37 mg/L	20.96 mg/L	23.2 mg/L	
[NO ₃]	n.m.	n.m.	n.m.	< D.L.
[HCO ₃]	n.m.	n.m.	n.m.	3.0 mg/L
[B]	306.5 ± 212.5 µg/L	146.1 µg/L	885 µg/L	

n.m. not measured; D.L. detection limit.

colloidal phases (e.g. Tc(IV) eigencolloids) and dissolved species a phase separation by ultracentrifugation (Beckman Optima XL 90, 90,000 rpm, 694,000 × g) for 1 h was applied. Redox potential of selected samples was measured in the Ar glovebox by using a Metrohm (Ag/AgCl, KCl (3 M)) Pt electrode. The measurements were performed directly in the sample without phase separation. The Eh values were recorded every hour and then corrected for the standard hydrogen potential (Eh always denotes corrected Eh_{SHE} in this work). The Eh values were recorded after ca. 1 h contact time. The redox potential measurements in the sorption experiments samples were carried out after about two weeks and 1 month contact time, respectively. Every sample was measured over a period of one day in the open vial in the Ar glovebox (<1 ppm O₂) to monitor the Eh evolution. A typical time dependent Eh evolution is shown in Fig. 1. The initial drop in Eh is likely due to the equilibration of the electrode with the solution, whereas the continuous drift to more oxidizing potentials in the later period might be

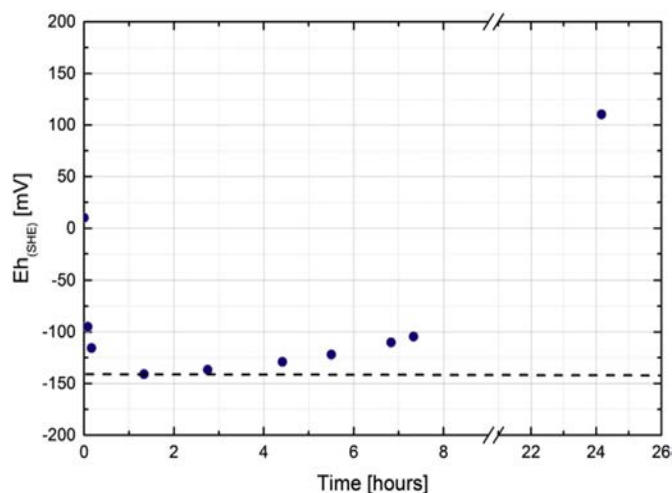


Fig. 1. Typical evolution for Eh measurement in synthetic Aspo groundwater simulant with un-oxidized diorite sample ([Tc] = 10⁻¹⁰ M). Dashed line marks the Eh value chosen as the final one.

explained to be a result of oxidation due to traces of oxygen in the Ar glovebox (<1 ppm O₂) that seems to be enough to compensate the redox capacity of the sample within 24 h. Therefore, the lowest Eh value detected was used as most representative for the undisturbed rock/water system in the closed vials.

2.4.2. Desorption experiments

Subsequent to the sorption kinetic experiments, desorption kinetic studies have been conducted. The Tc containing supernatant of the sorption experiment samples (samples with 3 months contact time in the sorption kinetic experiments) was removed and 8 mL of fresh Tc free groundwater added (natural AGW and Grimsel groundwater (glacial meltwater analogue)). For each contact time, the supernatant was always completely removed, analysed by LSC and substituted with fresh Tc free groundwater of the same volume. A subset of the samples was oxidized under air for one month after the sorption experiments. For this, the initial Tc containing liquid phase was removed and dry material in the vial was exposed to air before the fresh Tc free groundwater was added under aerobic atmosphere. For this experiment AGWS was used instead of natural AGW to keep oxidizing conditions. Desorption experiments cover a time range between a few seconds and 1 month contact time.

2.5. X ray spectroscopy

2.5.1. X ray photoelectron spectroscopy (XPS)

To examine the Tc surface speciation X ray photoelectron spectroscopy (XPS) was applied. For XPS analysis small un-oxidized Aspo diorite fragments with unpolished faces after cutting by circular saw were contacted with 10⁻⁵ M Tc(VII) in AGWS for two months and washed by MilliQ water for a few seconds to prevent salt precipitation directly before the XPS analysis. All preparation and measurement steps were performed under Ar atmosphere. Transport of the samples from the Ar glovebox to the XPS spectrometer under anoxic atmosphere was achieved by using an O ring sealed vacuum transfer vessel (PHI model 04 110). XPS measurements were carried out with the XPS system PHI 5000

VersaProbe II (ULVAC PHI Inc.) equipped with a scanning micro probe X ray source (monochromatic Al K α (1486.7 eV) X rays) in combination with an electron flood gun and a floating ion gun generating low energy electrons (1.1 eV) and low energy argon ions (8 eV) for charge compensation at isolating samples (dual beam technique), respectively. The angle between sample surface and analyser was set to 45°. Survey scans were recorded with an X ray source power of 12 W and pass energy of 187.85 eV. Narrow scans of the elemental lines were recorded at 23.5 eV pass energy. All spectra were charge referenced to C 1s (hydrocarbon) at 284.8 eV. Data analysis was performed using ULVAC PHI MultiPak program, version 9.5.

2.5.2. X ray absorption spectroscopy (XAS)

XAS experiments were performed at the INE Beamline at the ANKA 2.5 GeV synchrotron radiation facility, Karlsruhe Institute of Technology (KIT), Karlsruhe, Germany. The detailed description of the instrumental setup of the INE beamline is presented in Rothe et al. (2012). Tc K edge (21,044 eV) X ray absorption near edge structure (XANES) spectra were collected in fluorescence mode using one element VITUS Vacuum Silicon Drift Detector (SDD, Munich, Germany). The uranium mineral meta schoepite (UO $_3$ ·nH $_2$ O) was measured simultaneously with all samples and the Tc(IV) and Tc(VII) references. Per technetate solution with concentration of 10 $^{-2}$ M was taken as a Tc(VII) reference and TcO $_2$ × 1.6H $_2$ O(s) solid phase was prepared by TcO $_4^-$ reduction in the electrochemical cell and used as Tc(IV) reference. The U L $_2$ (20,948 eV) edge XANES spectra were used for energy calibration. The set of samples with Tc concentrations of \approx 10 $^{-3}$ M contacted with crystalline rock materials was prepared and mounted in an inert gas cell under argon atmosphere (see Table 3 for an overview of all XAS samples and references measured). During the measurements, argon continually flowed through the cell. Data reduction and normalization was performed with the ATHENA program part of the IFEFFIT software package (Ravel and Newville, 2005).

2.6. Thermodynamic modelling

Geochemical speciation calculations and sorption modelling were conducted with the geochemical speciation code PHREEQC (version 2) (Parkhurst and Appelo, 1999). The SIT database provided with PHREEQC is used, in which the thermodynamic constants for Tc correspond to the ones selected by the NEA Thermochemical Database (Guillaumont et al., 2003). Pourbaix diagrams were calculated and plotted with "Geochemist's Workbench" (version 8.0, Aqueous Solution LLC) code with the default database ther.mo.dat also modified for Tc species in accordance with NEA Thermochemical Database (Guillaumont et al., 2003).

Under the applied experimental conditions TcO $_4^-$ and TcO(OH) $_2$ are the only relevant dissolved species for Tc(VII) and Tc(IV), respectively. The redox reaction is:

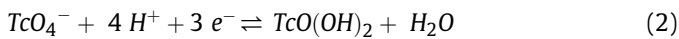


Table 3
List of samples studied by XAS.

Sample	[Tc], M	Description
Tc(VII) reference	0.01	TcO $_4^-$ solution
Tc(IV) reference		Solid TcO $_2$ covered with supernatant
Tc on AD	0.001	Centrifuged suspension

$$K_{\text{VII/IV}} = \frac{[\text{TcO(OH)}_2]}{[\text{TcO}_4^-][\text{H}^+]^4[\text{e}^-]^3} \quad (3)$$

where $K_{\text{VII/IV}}$ is the conditional constant of reaction (2) at a given ionic strength. From here the pe (pe = $\log a_e$ = 16.9 × Eh at 25 °C) is calculated according to the following equation:

$$\text{pe} = \left(\log K_{\text{VII/IV}} + \log \left(\frac{[\text{TcO}_4^-]}{[\text{TcO(OH)}_2]} \right) - 4\text{pH}_c \right) / 3 \quad (4)$$

where $\text{pH}_c = \log [\text{H}^+]$. The pe corresponding to the 50/50% Tc(VII)/Tc(IV) borderline on a Pourbaix diagram pertaining only to the aqueous species (denoted pe_{aq} or Eh_{aq} for redox potential) is found as follows:

$$\text{pe}_{\text{aq}} = \left(\log K_{\text{VII/IV}} - 4\text{pH}_c \right) / 3 \quad (5)$$

Sorption of Tc(IV) onto mineral surfaces can also be taken into account. Because this study is restricted to pH \approx 8 and low ionic strength for the sorption studies, no surface site protolysis or electrostatics are taken into account. We have considered the following simple reaction (6) to describe sorption onto the mineral surface:



where $\equiv\text{S}$ is a generic surface site and $[\equiv\text{S}]$ can be calculated using equation (7) with the following parameters: site density: 1 site/nm 2 ; surface area: 0.16 m 2 /g; S/V: 250 g/L.

$$[\equiv\text{S}] = \text{site density} \times \text{surface area} \times (S/V) / N_A \\ 6.64 \times 10^{-5} \text{ mol/L} \quad (7)$$

where N_A is the Avogadro constant. A similar surface complexation approach was proposed by Cui and Eriksen (1996) for Tc uptake by Fe(II) bearing minerals. According to the reaction (6) the reaction constant is calculated as (8):

$$K_{\text{VII/IV,surf}} = \frac{[\equiv\text{STcO(OH)}_2]}{[\equiv\text{S}][\text{TcO}_4^-][\text{H}^+]^4[\text{e}^-]^3} \quad (8)$$

Tc(IV) uptake on mineral surfaces is high (Westsik et al., 2014), so $[\equiv\text{STcO(OH)}_2]$ is expected to be much larger than $[\text{TcO(OH)}_2]_{\text{(aq)}}$. By contrast, Tc(VII) uptake on minerals can be neglected (Wildung et al., 2004). Using the surface complexation model, the Tc(VII)/Tc(IV) borderline on a Pourbaix diagram accounting for both processes in solution and at the mineral surfaces (denoted pe_{surf} or Eh_{surf}) is calculated as follows:

$$\text{pe} = \left(\log K_{\text{VII/IV,surf}} + \log \left(\frac{[\text{TcO}_4^-]}{[\equiv\text{STcO(OH)}_2]} \right) - 4\text{pH}_c + \log[\equiv\text{S}] \right) \\ \times / 3 \quad (9)$$

$$\text{pe}_{\text{surf}} = \left(\log K_{\text{VII/IV,surf}} - 4\text{pH}_c + \log[\equiv\text{S}] \right) / 3 \quad (10)$$

In other words, pe_{surf} is the pe value for 50% Tc uptake. Equation (10) applies only for sufficiently low $[\text{Tc}]_{\text{tot}}$ or high Eh , i.e. where the precipitation of TcO $_2$ ·1.6H $_2$ O(s) does not occur. Note that, in a

modelling study of plutonium (Pu) uptake on kaolinite (Marsac et al., 2015a), calculated borderlines between two Pu oxidation states pertaining only to the speciation at the kaolinite surface. Such type of calculation cannot be made in our study because Tc(VII) uptake on minerals is unlikely to be quantifiable, in contrast to the relevant Pu oxidation states.

3. Results

3.1. Batch sorption studies

3.1.1. Sorption on Aspo diorite

In the following the term “sorption” implies the total Tc uptake by the solid phase independent of the underlying process (sorption only or reductive sorption). Time dependent sorption of different Tc(VII) concentrations onto oxidized and un oxidized AD are given in Fig. 2 for $[Tc]_{tot} = 10^{-5}$ M (Fig. 2a), 10^{-8} M (Fig. 2b), and 10^{-9} M (Fig. 2c). From the Tc sorption kinetic experiments, it is evident that Tc uptake on un oxidized material is much higher than the artificially oxidized one. For the sample series of 10^{-8} M and 10^{-9} M $[Tc]_{tot}$ on an oxidized material plateau values close to 100% sorption are obtained (after 90 days contact time), whereas during the same observation period in experiments with oxidized AD only $\approx 40\%$ are removed from solution. Reaching the plateau value for Tc uptake takes more time at lower $[Tc]_{tot}$ concentration. In samples with 10^{-5} M Tc much less relative uptake is observed showing a plateau level for sorbed Tc of around 20–25% for the un oxidized samples and $\approx 10\%$ for the oxidized samples. The steady state is reached after approximately seven days which is much faster than observed for experiments with lower $[Tc]_{tot}$.

The formation of colloidal Tc phases (eigencolloids) examined by comparison of Tc concentration in ultracentrifuged to non ultracentrifuged samples was not detectable within the uncertainty limits (± 5 –10%). Either these colloidal phases are not formed or are not stable under the Aspo GWS conditions chosen (ionic strength ≈ 0.2 M, pH 8).

Redox potential measurements of Tc containing AGWS after two weeks and 1 month equilibration time with oxidized and un oxidized AD for three different $[Tc]_{tot}$ are shown in Fig. 3, together with Pourbaix diagrams calculated for the AGW composition. For the oxidized AD material the redox potential (E_{SHE}) does not change significantly as a function of Tc concentration and is within the range of +230 to +280 mV. However, for un oxidized AD material two trends were observed during the Eh measurements: (a) for low Tc concentration (up to 10^{-8} M) the Eh value decreases with time from 14 days to one month and (b) for the highest Tc

concentration used (10^{-5} M) the Eh value was unchanged within the analytical uncertainty. Based on the measured redox potentials in combination with thermodynamic considerations the following conclusions can be drawn (at least after 2 weeks contact time): (i) for $[Tc] = 10^{-9}$ M Tc(VII) is reduced to a Tc(IV) species in solution whereas (ii) for $[Tc] = 10^{-8}$ M Tc(IV) precipitates as a solid phase. In case of Tc 10^{-5} M (iii) Tc(VII) might not be fully reduced to Tc(IV) since the measured E_{SHE} values are above the borderline. Nevertheless, a fraction of Tc(VII) might be reduced since the borderline represents already 50%/50% Tc(VII)/Tc(IV). In this case the reduced Tc precipitates as a Tc(IV) solid phase.

3.2. Desorption studies

3.2.1. Desorption experiments without artificial oxidation

Tc desorption was experimentally monitored over one month using sorption samples for which Tc had been previously equilibrated with rock material for three months. Very low Tc desorption was observed in all cases studied irrespective of the nature of the material (oxidized or un oxidized) used for sorption. For the case of AD samples two types of natural groundwater were used, namely Aspo and Grimsel GWs (representing glacial melt water composition with low ionic strength, see Table 2). Tc was detected in the liquid phase only for samples after contact with 10^{-5} M Tc AGWS (Fig. 4). After 1 day contact time desorption achieved values of up to 7% of the Tc amount sorbed after the uptake studies. This level remained relatively stable up to 30 days of contact time. For lower Tc concentrations (10^{-8} M and 10^{-9} M initial concentration for sorption experiments) no desorption was detected with the detection limit of the analytical method.

3.2.2. Desorption experiments with artificial oxidation

Desorption kinetics for AD with different $[Tc]_{initial}$ after sample pre oxidation is given in Fig. 4. Pre oxidation of the AD samples under aerobic conditions for 1 month before addition of AGWS changed the Tc desorption behaviour drastically (Fig. 4). Both sorption experiments with originally oxidized and un oxidized materials revealed the same desorption behaviour. Desorption is fast with the main part of technetium being released after a few seconds contact time and after one day a concentration plateau value was reached.

3.3. Spectroscopic analyses

3.3.1. X ray photoelectron spectroscopy (XPS)

XPS analysis of an un oxidized AD disc fragment after contacting

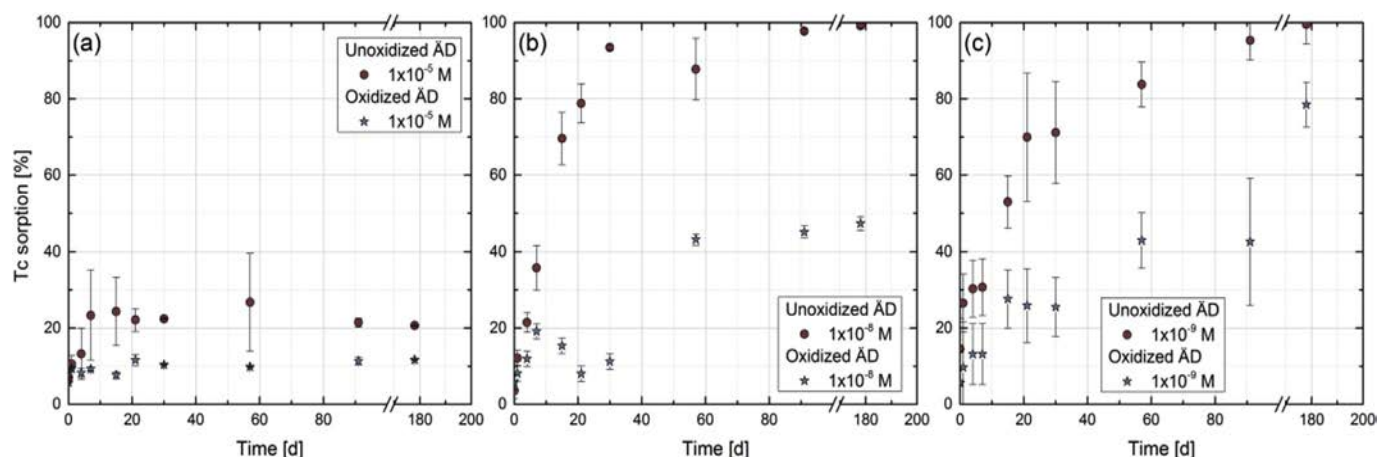


Fig. 2. Tc sorption kinetics for different Tc concentrations in presence of oxidized and un-oxidized AD (pH 8, I = 0.2 M).

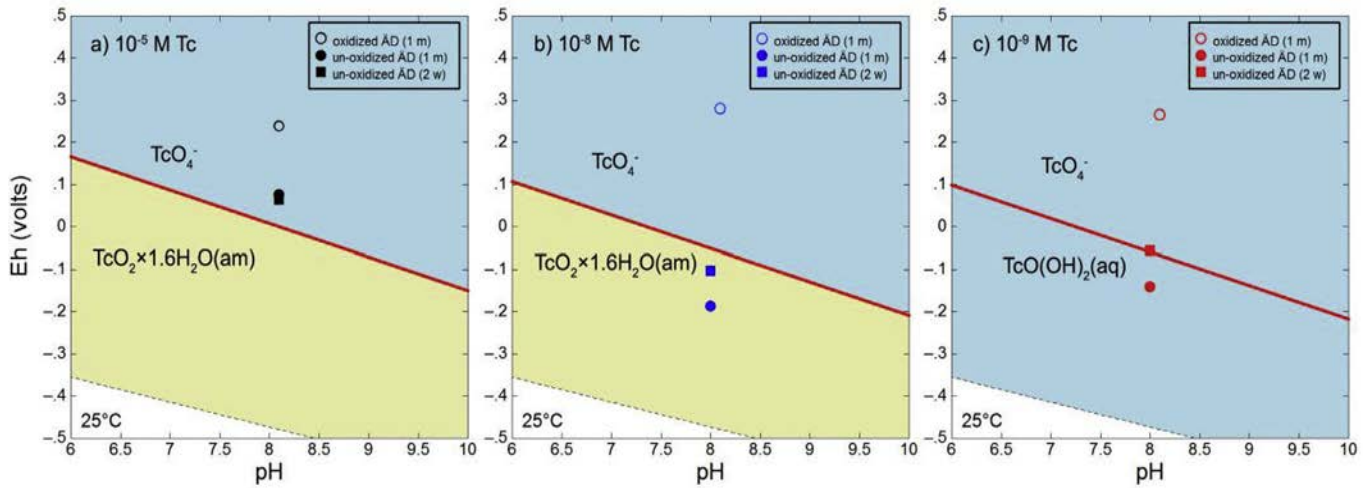


Fig. 3. Pourbaix diagrams for AGWS containing different Tc concentrations: (a) 10^{-5} M, (b) 10^{-8} M, and (c) 10^{-9} M. Data points are given for oxidized (open symbols) and un-oxidized (filled symbols) AD for a contact time of two weeks (squares) and one month (circles).

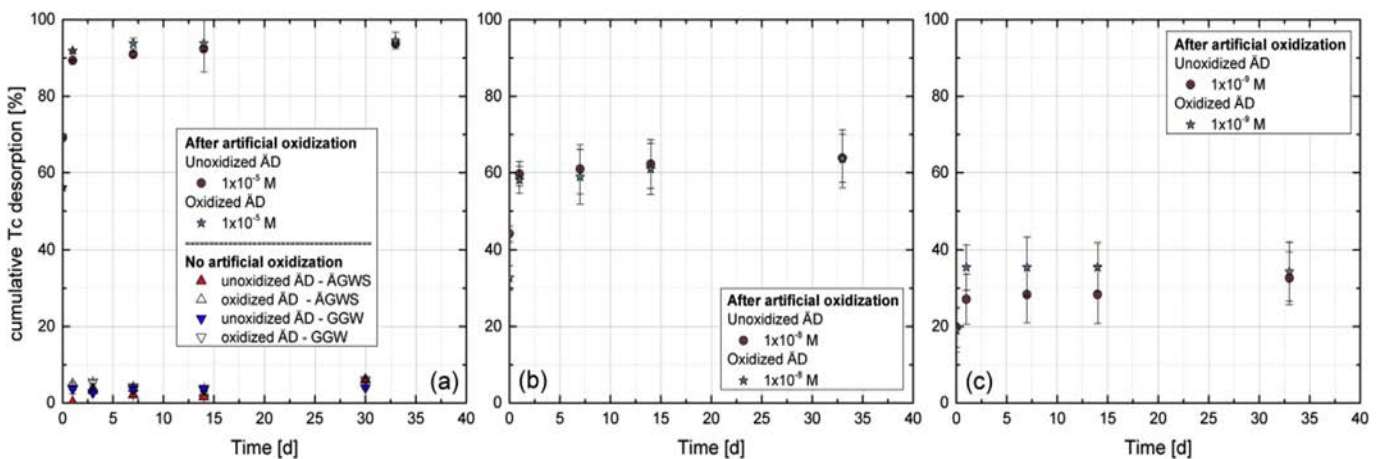


Fig. 4. Desorption of Tc sorbed to oxidized and un-oxidized AD material by AGWS after 1 month pre-oxidation under atmospheric conditions. Results of the experiment after artificial oxidation and contact with AGWS and GGW are additionally included in (a). Please note that these data points have the unit “% desorbed”.

with 10^{-5} M Tc(VII) in AGWS for 2 months under Ar atmosphere in the glovebox revealed that Tc is associated to mafic (dark) minerals only (see Figure A2), whereas on felsic (light) minerals no Tc was found. Fig. 5 (left) shows the measured Tc 3d XPS spectrum with the characteristic $3d_{3/2}$ and $3d_{5/2}$ peak positions. Due to the rather low Tc concentration used in the sorption experiment on the AD disc the spectrum is quite noisy. Both Tc(VII) and Tc(IV) should have two 3d peaks ($3d_{5/2}$ and $3d_{3/2}$) for each oxidation state. Since there are only two peaks in the area of interest, the conclusion is that there is only one Tc oxidation state present at the mineral surface, and the binding energy of the Tc(IV) $3d_{5/2}$ (TcO_2) reference line at 256.8 eV is closer to the experimental data (255.9 eV) than the Tc(VII) $3d_{5/2}$ (NaTcO_4) 259.7 eV reference line. It was therefore concluded that Tc found on the AD surface is in the tetravalent oxidation state. Binding energy reference lines for TcO_2 and NaTcO_4 were taken from Wester et al. (1987).

3.3.2. X ray absorption near edge structure (XANES)

XANES analysis provides bulk information on the Tc oxidation states after interaction of 10^{-3} M Tc with AD. Normalized Tc K edge XANES spectra are presented in Fig. 5 (right) for Tc on AD together with Tc(IV) and Tc(VII) references. The Tc K edge XANES spectra of the TcO_2 and TcO_4^- reference materials have characteristic features, which readily allow Tc oxidation state characterization. For

example, the spectrum of the Tc(VII) reference, where Tc is surrounded by four oxygen atoms in tetrahedral configuration, exhibits a pre edge absorption resonance at about 21,050 eV generated by the $1s \rightarrow 5p/4d$ transition (Altmaier et al., 2011b). Since Tc(IV) generally possesses octahedral coordination, this transition is forbidden and the pre edge feature cannot be seen in the spectrum of the Tc(IV) reference compound. The overall shape and energy position of the rising absorption edge of the Tc K edge XANES spectrum of Tc on Aspo diorite is similar to the TcO_2 reference without the pre edge feature of Tc(VII). These fingerprint approach allows to identify Tc(IV) as dominating Tc species on AD in line with the XPS results.

4. Discussions

4.1. Tc uptake mechanisms

The spectroscopic investigations described above together with the batch sorption/desorption experimental results and the thermodynamic calculations demonstrate that Tc retention in a reducing condition is always coupled to a reduction process from Tc(VII) to Tc(IV). Tc(VII) shows no or only very weak sorption. Thus, the mechanism leading to the removal of Tc from solution may be attributed to (i) a sorption/surface complexation of a Tc(IV) species

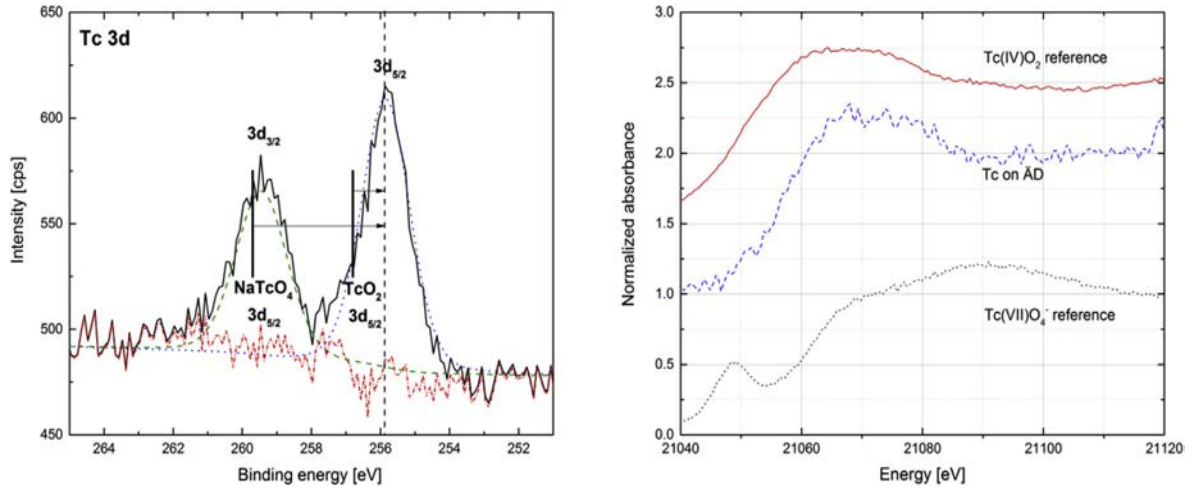


Fig. 5. (Left) Tc 3d XPS narrow scan spectrum of an AD sample after contacting with Tc(VII)-containing AGWS. The green (dashed) and blue (dotted) curves show the fits to the $3d_{3/2}$ and $3d_{5/2}$ XPS elemental lines, respectively, the red line represents the residuum. (Right) Normalized Tc K-edge XANES spectra of a sample after sorption of Tc onto AD and of Tc(IV) and Tc(VII) references.

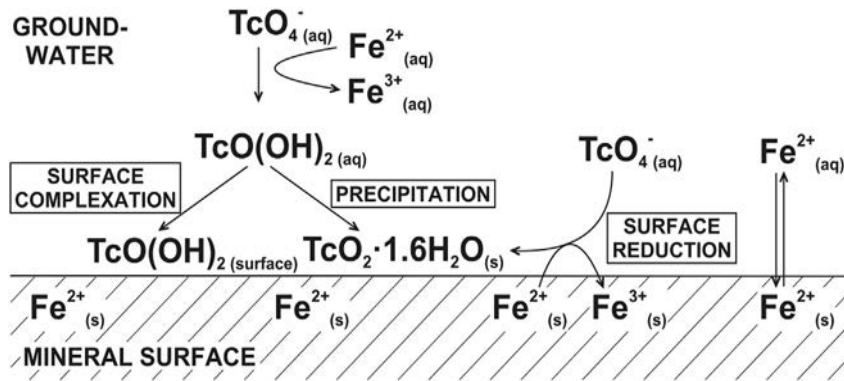
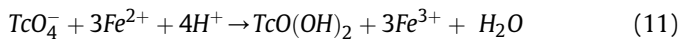


Fig. 6. General scheme of Tc(VII) sorption and reduction processes.

after reduction in solution by e.g. dissolved Fe(II) and/or (ii) precipitation of poorly soluble $TcO_2 \cdot 1.6H_2O_{(s)}$ again due to Tc(VII) reduction in solution by e.g. dissolved Fe(II) species. Especially in those experiments with the highest Tc concentration a reduction/precipitation process might occur, as the Tc(IV) solubility limit of 4.4×10^{-9} M (Duro et al., 2006) should be significantly exceeded in case of reduction. A third possible mechanism of Tc retention could be (iii) the Tc(VII) reduction by structurally bound or surface bound Fe(II) species. A general scheme of the processes potentially involved into Tc(VII) immobilization is shown in Fig. 6.

Considering only Fe(II) as a potential reducing agent for Tc(VII)/Tc(IV) the transformation follows according to equation (11):



In a first attempt we tried to assess whether the available amount of Fe(II) is sufficient to reduce added Tc(VII). The ion exchangeable Fe(II) content was taken as an approximation for the readily “available Fe(II)” and decreases from $(2.2 \pm 0.5) \times 10^{-5}$ M in an oxidized AD to $(9 \pm 5) \times 10^{-6}$ M in oxidized AD. Based on the solid to liquid ratio chosen (250 g/L) these values give $(1.8 \pm 0.4) \times 10^{-7}$ mol/vial Fe(II) for un oxidized AD and $(7 \pm 4) \times 10^{-8}$ mol/vial Fe(II) for oxidized AD. Thus, it is obvious that the material extracted and transferred under normal ambient atmospheric conditions (oxidized AD) possesses a lower redox capacity. From the comparison of the Fe(II) content ($(7 \pm 4) \times 10^{-8}$ mol/vial Fe(II)) with the total amount of added Tc

(8×10^{-8} mol/vial (10^{-5} M Tc), 8×10^{-11} mol/vial (10^{-8} M Tc), and 8×10^{-12} mol/vial (10^{-9} M Tc)) and taking into account that three electrons are required to reduce Tc(VII) to Tc(IV) oxidized AD still provides enough ion exchangeable Fe(II) to reduce $29 \pm 17\%$ of total Tc in the sample containing 10^{-5} M Tc, which is close to the experimental observation of $12 \pm 1\%$ Tc being reduced. Furthermore, an oxidized AD does not provide enough Fe(II) for the complete reduction of 10^{-5} M Tc. These estimations are supported by the finding that Eh values in the granite/water suspensions increase significantly when 10^{-5} M Tc(VII) added. This amount is apparently sufficient to exceed the redox capacity of the diorite material at a solid to liquid ratio of 250 g/L. In all batch experiments the granite material should provide enough Fe(II) for the Tc(VII) reduction at $[Tc]_{tot} < 10^{-8}$ M.

4.2. Sorption parameters

The temporal change in Tc concentration during the batch sorption experiment can be described with an exponential decay equation (12):

$$C_t = (C_0 - C_{eq})e^{-kt} + C_{eq} \quad (12)$$

where C_0 and C_{eq} are the initial and equilibrium Tc concentrations (M), respectively, and k is the sorption rate coefficient (time^{-1}). Hence, calculating sorption S_t as (13)

$$S_t = \left(1 - \frac{C_t}{C_0}\right) \times 100\% \quad (13)$$

time dependent sorption data can be fitted with the rate equation (14):

$$S_t = S_{eq} \left(1 - e^{-kt}\right) \quad (14)$$

where S_t and S_{eq} are the sorption percentages at the moment t and at equilibrium (6 months contact time), respectively. Sorption rate coefficients obtained from this fitting are presented in Table 4. The uptake rates (k) are significantly higher for the experiments with high total Tc concentration, which is a general observation in chemical reaction kinetics. A closer inspection shows that fitting of experimental data obtained with highest Tc concentrations to the kinetic rate model provides a better agreement when two exponential functions (rate constants) are taken. For instance, the sorption of 10^{-5} M Tc onto oxidized AD can be fitted with two exponential functions with k values of 0.017 ± 0.008 and 0.265 ± 0.056 d^{-1} . This might be an indication of the existence of more than one retention mechanism, e.g. surface sorption and precipitation, respectively. We have to emphasize, however, that the system consists of highly coupled redox, precipitation and surface interaction phenomena. A simple interpretation of sorption mechanisms just based on reaction rate analysis is certainly not feasible. This becomes obvious when looking to literature data. Exponential fitting of Tc sorption data by Bondietti and Francis (1979) gives a k value of around 1.1 ± 0.4 d^{-1} for an initial Tc concentration of 1.1×10^{-7} M with Westerly granite as a solid material (167 g/L solid to liquid ratio). The pH/Eh values for this material were also comparable (pH 8, Eh 100 mV) to the conditions used in the present work, but neither Fe(II) content nor specific surface area of the material were specified in the paper, which could significantly contribute to the enhanced rates found in Bondietti and Francis (1979).

Distribution coefficients (K_d in L/kg) obtained for Tc sorption onto Aspo material were calculated using the following equation (15):

$$K_d = \frac{C_l}{C_s} \frac{A_0 - A_l}{A_l} \times \frac{V}{m_{solid}} \quad (15)$$

where C_l and C_s are the equilibrium concentrations of solutes in aqueous and solid phases, respectively, A_0 and A_l are the initial and final aqueous radionuclide activities at equilibrium (Bq/mL), respectively, V is the volume of the aqueous phase (mL) and m_{solid} is the solid mass (g). Typical K_d values obtained within the present work are presented in Table 4 together with measured initial Tc concentrations, amount of ion exchangeable Fe(II) and redox potentials. From a thermodynamic point of view the K_d approach assumes a fully reversible sorption process, but in most papers it is

Table 4
Main parameters obtained by Tc(VII) sorption experiments onto AD.

Material	Fe(II) available, mg/g	Initial Tc concentration, mol/L	Eh _(SHE) , after 1 2 months ^a , mV	k , d^{-1}	K_d , L/kg	K_a , m	Tc sorbed after 6 months, %
AD un-oxidized	4 6	1.07×10^{-5}	76	0.24 ± 0.100	1.1 ± 0.200	$(6.8 \pm 0.8) \times 10^{-6}$	21 ± 2.0
		$(1.05 \pm 0.05) \times 10^{-8}$	-187	0.075 ± 0.009	500 ± 200	$(2.9 \pm 1.3) \times 10^{-3}$	99.2 ± 0.6
		$(1.10 \pm 0.10) \times 10^{-9}$	-142	0.036 ± 0.004	900 ± 800	$(5.3 \pm 4.9) \times 10^{-3}$	99.5 ± 6.0
AD oxidized	1 3	1.07×10^{-5}	238	0.15 ± 0.040	0.53 ± 0.050	$(3.3 \pm 0.3) \times 10^{-6}$	12 ± 1.0
		$(1.05 \pm 0.05) \times 10^{-8}$	280	0.017 ± 0.010	3.6 ± 1.000	$(2.2 \pm 0.6) \times 10^{-5}$	47 ± 8.0
		$(1.10 \pm 0.10) \times 10^{-9}$	264	0.007 ± 0.001	22 ± 8	$(1.4 \pm 0.5) \times 10^{-4}$	84 ± 6.0

^a Values in Fig. 3; N/A not applicable.

used even when irreversible reduction/precipitation processes are involved (Albinsson et al., 1991; Allard et al., 1979; Kaplan and Serne, 1998). In the report of USEPA (1999) authors describe "conditional" K_d values for the interpretation of experimental data in cases when the rigorous application of the K_d approach is prohibited (e.g. in non equilibrium, irreversible, or solubility controlled systems). In the present work K_d values are considered as conditional distribution coefficients. For a better comparison of the retention behaviour with literature data, K_d should be normalized to the specific surface area of the solid material used in the experiments according to equation (16):

$$K_a = \frac{K_d}{S_{BET}} \left(\times 10^{-6}\right) \quad (16)$$

where K_a is the surface area normalized distribution coefficient (m) and S_{BET} is the specific surface area of the solid determined by N_2 BET (m^2/g). K_a values for the AD material are shown in Table 4. Since the surface area of oxidized and un oxidized AD remains the same, this normalization does not affect the comparison between them. The K_d values obtained for the oxidized material (see Table 4; 10^{-5} M Tc) in this study with 0.53 ± 0.05 L/kg for oxidized AD are in good agreement with recently published data of Videnska and Havlova (2012) who reported a K_d value of 0.3 L/kg under oxidizing conditions for 1.6×10^{-4} M ^{99m}Tc on granitic rocks from Melechov Massive, Centre Bohemian Massive, Czech Republic (> 0.8 mm size fraction). Since the surface area was not mentioned in the publication, K_a values cannot be calculated for these results. Batch type studies on Tc uptake with well preserved un oxidized crushed granitic rocks can hardly be found in the literature. We have compared the data obtained with experiments performed under artificial reducing conditions. Ito and Kanno (1988) have published the Tc distribution between solution and granitic rocks (0.49–0.83 mm size fraction, 10^{-12} M [^{99m}Tc]) together with a number of other minerals under oxidizing and reducing conditions. Under oxidizing conditions (in 0.16 M NaNO₃) K_d values of 0.1 L/kg ($K_a = 4.8 \times 10^{-7}$ m) were obtained, while under reducing conditions (0.1 M NaBH₄ and 0.16 M NaNO₃) values of 45.6 L/kg ($K_a = 2.2 \times 10^{-4}$ m) increasing up to 68 L/kg ($K_a = 3.2 \times 10^{-4}$ m) with decreasing NO₃⁻ concentration down to 0.016 M could be determined. The paper by McKinley and Scholtis (1993) summarized the data on K_d values of Tc on different materials including granitic rocks used for the safety assessment of waste disposal at that time. Here the values range from 0 to 250 L/kg depending on the experimental conditions and the origin of the rocks. The authors emphasize that Tc sorption under oxidizing conditions is normally very low or zero, and for reducing conditions K_d values increase by 1–2 orders of magnitude.

4.3. Tc desorption

As was shown in the results section, Tc desorption without

artificial oxidation of the material is almost negligible. We suppose that the relatively rapid establishment of a steady state for the Tc concentration after only 1 day desorption is the consequence of washing out residual Tc(VII) in the porewater rather than desorption of sorbed or precipitated Tc(IV). For the desorption experiments after artificial oxidation, the general trend of the fast desorption up to a plateau value might be explained by the rapid oxidation of surface associated Tc(IV) to the heptavalent oxidation state and thus to the (almost) non sorbing pertechnetate anion whereas strongly sorbing un oxidized Tc(IV) does not have any significant contribution to the desorption process. The same observations were made by numerous investigators (Begg et al., 2008; Burke et al., 2006; Morris et al., 2008), where Tc(IV) oxidation to Tc(VII) was found to be a driving force for the Tc desorption process. Taking into account Tc uptake mechanisms discussed in section 4.1, one can assume two different mechanisms, namely predominantly surface complexation for $\log [Tc]_{tot} \leq 8$ and $TcO_2 \cdot 1.6H_2O_{(s)}$ precipitation for $\log [Tc]_{tot} > 5$ governing the Tc surface association process. Consequently, for the same initial Tc concentration, a similar Tc desorption behaviour can be expected for oxidized and un oxidized systems, which is in a good agreement with the experimental data observed for the AD. A higher degree of desorption observed for the samples with higher $[Tc]_{initial}$ might be explained by the relatively easier oxidation of the surface associated $TcO_2 \cdot 1.6H_2O_{(s)}$ phase in comparison to the surface complexed Tc(IV) species (see Table 5) which are probably more recalcitrant to remobilization during oxidation. Similar presumptions were expressed (Begg et al., 2008; Burke et al., 2006; Morris et al., 2008), but the mechanistical nature of this resistance is still a matter of further research.

4.4. Spectroscopic analyses

According to the XPS results (see Fig. 5 left), the Tc signal was detected only on dark mica type mineral surface (most likely biotite or magnetite), which contains structural Fe(II). It is well known that Tc(VII) is concentrated on Fe(II) containing minerals (Burke et al., 2010; Fredrickson et al., 2009; McBeth et al., 2011) as "hot spots" due to surface (heterogeneous) reduction into insoluble Tc(IV) oxide phase or/and homogeneous reduction in the solution into soluble Tc(IV) species with subsequent sorption on the mineral surface. According to the results of Peretyazhko et al. (2008a) heterogeneous Tc(VII) reduction on the surface associated Fe(II) is orders of magnitude faster than the homogeneous reduction by aqueous Fe^{2+} and may occur on the Fe(II) containing mineral surfaces. XANES analysis of the Aspo diorite contacted with Tc containing AGWS indicated the presence of Tc(IV) as well.

4.5. Thermodynamic modelling

The general scheme of the modelling applied is described in Section 2.6. A similar calculation approach was applied in previous studies related to the modelling of Pu sorption to kaolinite (Marsac

et al., 2015a) and Np sorption on illite (Marsac et al., 2015b) with respect to the differences in chemistry. Fig. 7 shows the Tc(IV) fraction in the aqueous phase modelled with PHREEQC for $\log [Tc]_{tot} \leq 8$ as a function of the redox potential. For pH 8.0 and $I = 0.1$ M, Eh of the $[Tc(VII)]_{aq}/[Tc(IV)]_{aq}$ borderline is 53 mV (E_{haq} , calculated from equation (5)), as highlighted in Fig. 7. To account for sorption processes (see equation (9)), $\log K_{VII/IV,surf}$ is determined as follows. The site density is arbitrarily set equal to 1 site/nm², which is the same order of magnitude as commonly observed for several minerals (Burlakov et al., 2000; Jeppu and Clement, 2012). The value for $\log K_{VII/IV,surf}$ is strongly dependent on this arbitrarily chosen site density. At Eh values ≤ 90 mV almost all Tc is calculated to be Tc(IV) (see Fig. 7). Such conditions prevail in the experiments with un oxidized AD and $\log [Tc]_{tot} \leq 8$. Taking these experimental data, $\log K_{VII/IV,surf}$ is deduced by a fitting procedure and is found to be equal to 35.7 (see equation (8)). This value is kept constant for all the following calculations.

The borderline redox potential where $[Tc(IV)]_{surf}$ and $[Tc(VII)]_{aq}$ exist in equimolar concentrations, E_{hsurf} , is found equal to 12 mV in accordance to equation (10). In agreement with the findings of Marsac et al. (2015a, 2015b), for Np and Pu sorption to clays, the strong sorption behaviour of Tc(IV) shifts the borderline Eh to higher values as compared to that for the $[Tc(IV)]_{aq}/[Tc(VII)]_{aq}$ ratio, E_{haq} , in aqueous solution in the absence of mineral surfaces. For $\log [Tc]_{tot} > 5$ precipitation of $TcO_2 \cdot 1.6H_2O_{(s)}$ is predicted, which represents the 2nd retention mechanism, and extends the stability field of Tc(IV) further. In the respective experiment the measured Eh value (E_{hexp}) is $76 \text{ mV} \pm 50 \text{ mV}$, where the model predicts insignificant uptake in disagreement with the experimentally observed $\approx 21\%$ uptake. Actually, the model is very sensitive to the redox potential. For instance, a change in Tc uptake from 2% to 80% is predicted by assuming a slight decrease in E_{hcalc} from +20 to 0 mV for $\log [Tc]_{tot} = 5$. Regarding the uncertainties of experimental Eh data in a range of ± 50 mV (Altmaier et al., 2011a) and the uncertainty of model parameters, our simulation results are not so different from experimental data. The discrepancy of Tc uptake in simulation and experiment can easily be explained by uncertainties in redox potential measurements. According to model calculations, the dominating uptake mechanism at $\log [Tc]_{tot} = 5$ is

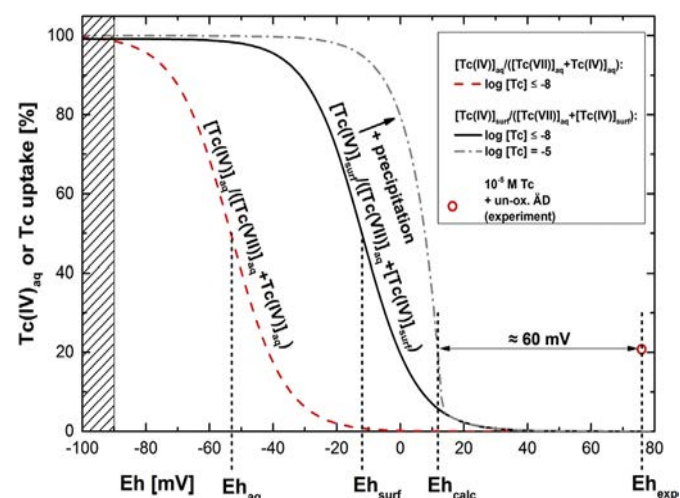


Fig. 7. Tc(IV) fractions depending on the redox potential (pH 8, $I = 0.1$ M) calculated according to equations (4) and (9), respectively. E_{hexp} corresponds to the measured redox potential; E_{hcalc} relates to the calculated redox potential where 21% of Tc is removed from solution in the experiment with $\log [Tc]_{tot} = 5$; $[Tc(VII)]_{aq}/[Tc(IV)]_{aq}$ and $[Tc(VII)]_{aq}/[Tc(IV)]_{surf}$ borderline redox potentials are as well marked by vertical dashed lines; the shaded area at the left side shows the Eh region where model calculations predict quantitative uptake.

Table 5

Comparison of the sorption/desorption values for the oxidized and un-oxidized AD for the artificially oxidized sample series. Desorption time of 1 month.

Material	$-\log [Tc]_{initial, M}$	Tc sorption, %	Tc desorption, %
AD (un-oxidized)	5	21 ± 2	93.7 ± 0.6
	8	99.2 ± 0.6	64 ± 7
	9	99.5 ± 0.6	33 ± 7
AD (oxidized)	5	12 ± 1	94 ± 3
	8	47 ± 8	64 ± 8
	9	84 ± 6	35 ± 8

precipitation of $\text{TcO}_2 \cdot 1.6\text{H}_2\text{O}_{(s)}$. This is in agreement with XANES measurements performed with a 1 mM Tc containing solution contacted with the crushed material. The model predicts almost 100% Tc uptake for $E_h \leq 90$ mV in accordance with the experimental results for an oxidized AD at $\log [\text{Tc}]_{\text{tot}} \leq 8$ M (see Table 4). However, relatively high Tc uptake ($> 30\%$, see Tables 4 and 5) of the oxidized materials at $\log [\text{Tc}]_{\text{tot}} \leq 8$ M and rather high E_h values (> 200 mV) cannot be explained by the thermodynamic model. No Tc reduction and no uptake is calculated above $E_h \geq \approx 30$ mV (see Fig. 7). Nevertheless, Tc uptake by the oxidized materials is significant but is lower as compared to that by the un oxidized AD (see Fig. 2). This finding may suggest that, although oxidized, a redox partner for the reduction of Tc(VII) to Tc(IV) is present in significant amounts, which, however, is not detected by the E_h measurements using a Pt electrode. Another aspect relates to the concentration of redox partners required for reproducible and thermodynamically defined redox potential measurements using a Pt electrode, which is proposed to be $\geq \approx 10^{-6}$ M (Grenthe et al., 1992). The ion exchangeable ferrous iron concentration in the oxidized rock materials lies very close to that minimum value of $(9 \pm 5) \times 10^{-6}$ M Fe(II) for oxidized AD. It seems likely that Fe(II) content available is quantitatively consumed during the Tc reduction process by oxidation to Fe(III) inhibiting a precise E_h determination by the platinum electrode. Thus a higher uncertainty in the E_h measurements and in the interpretation of the results needs to be considered for the higher $[\text{Tc}]_{\text{tot}}$ series and the oxidized AD.

5. Conclusions

A batch type sorption/desorption study on Tc interaction with crushed granitic rock material from the generic URL in Sweden (Aspo HRL) was performed. Part of the crushed material from Aspo HRL used in the experiments has been obtained and handled under anoxic conditions before and during the experiments thus representing to a great extent natural *in situ* rock material conditions (e.g. redox capacity) relevant to the far field environment of a repository in crystalline rock. According to the experimental findings, Tc(VII) is reduced under natural anoxic conditions to Tc(IV) followed by either precipitation of $\text{TcO}_2 \cdot 1.6\text{H}_2\text{O}_{(s)}$ or/and surface complexation of soluble Tc(IV) species on the rock surface. Comparison of samples after ultracentrifugation shows no detectable amount of Tc colloidal phase under simulated groundwater conditions applied. After contact of Tc(VII) containing groundwater simulants with crystalline rock materials, Tc(IV) species were detected on mafic mica type Fe containing minerals. Apparently, the Tc(VII) concentration directly influences the amount of Tc uptake on un oxidized and oxidized material, which can be correlated with the ion exchangeable Fe(II) buffer available (4–6 $\mu\text{g/g}$ for un oxidized AD and 1–3 $\mu\text{g/g}$ for oxidized AD). Tc behaviour on oxidized AD differs dramatically compared to un oxidized AD samples. In general, artificially oxidized rock material could retain approx. 2 times less Tc compared to un oxidized material. Distribution coefficients (K_d) and surface area normalized distribution coefficients (K_a) were determined for artificially oxidized and original un oxidized AD which serve as parameters for transport modelling or performance assessment modelling purposes. Technetium desorption from the AD is insignificant under anoxic conditions, but after artificial oxidation technetium mobility is increased due to re oxidation of Tc(IV) to Tc(VII). Such reactions might become relevant in scenarios where oxidized glacial melt water intrusion into a repository is considered. The similar Tc desorption behaviour from the initially oxidized and un oxidized AD samples indicates the same retention mechanism for both types of the material even taking into account the difference in the total uptake capacity. Samples from the batch sorption studies with

high $[\text{Tc}]_{\text{tot}}$ show increased desorption most probably due to faster re oxidation of the $\text{TcO}_2 \cdot 1.6\text{H}_2\text{O}_{(s)}$ precipitate in comparison to surface complexed Tc(IV) species. According to the thermodynamic calculations, for $\log [\text{Tc}] \leq 8$ Tc(IV) surface complexation is a predominant process of Tc immobilization, while at higher Tc concentration $\text{TcO}_2 \cdot 1.6\text{H}_2\text{O}_{(s)}$ precipitation plays the main role. This work clearly highlights the importance of using well preserved (un oxidized) natural materials for the reliable estimation of the interaction of redox sensitive elements with these solid phases. The difference in retention capacity between artificially oxidized and un oxidized material is highly significant. The data obtained gives important implications on the prediction of Tc behaviour under natural conditions for safety assessment of deep geological disposals of SNF and HLW in undisturbed and disturbed crystalline environments.

Acknowledgements

The research leading to these results has received funding from the Federal Ministry of Economics and Technology (BMWi) collaborative project VESPA (Behaviour of long lived fission and activation products in the near field of a repository and possible retention mechanisms) under contract N° 02 E 10800 and the European Union's European Atomic Energy Community's (Euratom) 7th Framework Programme FP7/2007 2011 under grant agreement N° 269658 (CP CROCK).

References

- Albinsson, Y., Christiansen-Satmark, B., Engkvist, I., Johansson, W., 1991. Transport of actinides and Tc through a bentonite backfill containing small quantities of iron or copper. *Radiochim. Acta* 52 3, 283–286.
- Allard, B., Kigatsi, H., Torstenfelt, B., 1979. Technetium – reduction and sorption in granitic bedrock. *Radiochem. Radioanal. Lett.* 37, 223–229.
- Altmaier, M., Gaona, X., Fellhauer, D., Buckau, G., 2011a. Intercomparison of Redox Determination Methods on Designed and Near-natural Aqueous Systems, FP 7 EURATOM Collaborative Project “Redox Phenomena Controlling Systems”. KIT Scientific Publishing.
- Altmaier, M., Kienzler, B., Duro, L., Grivé, M., Montoya, V., 2011b. In: 3rd Annual Workshop Proceedings of the Collaborative Project “Redox Phenomena Controlling Systems” (7th EC FP CP RECOSY). KIT INE.
- Begg, J.D.C., Burke, I.T., Charnock, J.M., Morris, K., 2008. Technetium reduction and reoxidation behaviour in Dounreay soils. *Radiochim. Acta* 96, 631–636.
- Bodin, J., Delay, F., de Marsily, G., 2003. Solute transport in a single fracture with negligible matrix permeability: 2. mathematical formalism. *Hydrogeol. J.* 11, 434–454.
- Bondiotti, E.A., Francis, C.W., 1979. Geologic migration potentials of Technetium-99 and Neptunium-237. *Science* 203, 1337–1340.
- Boyd, G.E., Larson, Q.V., Motta, E.E., 1960. Isolation of milligram quantities of long-lived technetium from neutron irradiated molybdenum. *J. Am. Chem. Soc.* 82, 809–815.
- Burke, I.T., Boothman, C., Lloyd, J.R., Livens, F.R., Charnock, J.M., McBeth, J.M., Mortimer, R.J.G., Morris, K., 2006. Reoxidation behavior of technetium, iron, and sulfur in Estuarine sediments. *Environ. Sci. Technol.* 40, 3529–3535.
- Burke, I.T., Livens, F.R., Lloyd, J.R., Brown, A.P., Law, G.T.W., McBeth, J.M., Ellis, B.L., Lawson, R.S., Morris, K., 2010. The fate of technetium in reduced estuarine sediments: combining direct and indirect analyses. *Appl. Geochem.* 25, 233–241.
- Burlakov, V.M., Sutton, A.P., Briggs, G.A.D., Tsukahara, Y., 2000. Simulation of porous Si and SiO_x layer growth. In: MSM (Ed.), *Technical Proceedings of the 2000 International Conference on Modeling and Simulation of Microsystems*. University of Oxford, UK, pp. 95–97.
- Byegård, J., Johansson, H., Skålberg, M., Tullborg, E.-L., 1998. The Interaction of Sorbing and Non-sorbing Tracers with Different Aspo Rock Types. Sorption and diffusion experiments in the laboratory scale.
- Close, P., Hornyak, E.J., Baak, T., Tillman, J.F., 1966. Potentiometric titration of micro amounts of iron(II) with very dilute cerium(IV) sulfate. *Microchem. J.* 10, 334–339.
- Cui, D., Eriksen, T.E., 1996. Reduction of pertechnetate in solution by heterogeneous

- electron transfer from Fe(II)-containing geological material. *Environ. Sci. Technol.* 30, 2263–2269.
- Duro, L., Grivé, M., Cera, E., Gaona, X., Domènech, C., Bruno, J., 2006. Determination and Assessment of the Concentration Limits to Be Used in SR-can. SKB.
- Fredrickson, J.K., Zachara, J.M., Plymale, A.E., Heald, S.M., McKinley, J.P., Kennedy, D.W., Liu, C., Nachimuthu, P., 2009. Oxidative dissolution potential of biogenic and abiogenic TcO₂ in subsurface sediments. *Geochim. Cosmochim. Acta* 73, 2299–2313.
- Grambow, B., 2008. Mobile fission and activation products in nuclear waste disposal. *J. Contam. Hydrol.* 102, 180–186.
- Grenthe, I., Stumm, W., Laaksoharju, M., Nilsson, A.C., Wikberg, P., 1992. Redox potentials and redox reactions in deep groundwater systems. *Chem. Geol.* 98, 131–150.
- Guillaumont, R., Fanghanel, T., Fuger, J., Grenthe, I., Neck, V., Palmer, D.A., Rand, M.H., 2003. Update on the Chemical Thermodynamics of Uranium, Neptunium, Plutonium, Americium and Technetium. Elsevier.
- Heald, S.M., Zachara, J.M., Jeon, B.H., McKinley, J.P., Kukkadapu, R., Moore, D., 2007. XAFS study of the chemical and structural states of technetium in Fe(III) oxide co-precipitates. *X-Ray Absorpt. Fine Structure-XAFS* 13, 882, 173–175.
- Heck, S., Schafer, T., 2012. Short Note: CP CROCK Groundwater Sample Characterization.
- Heron, G., Crouzet, C., Bourg, A.C.M., Christensen, T.H., 1994. Speciation of Fe(II) and Fe(III) in contaminated aquifer sediments using chemical extraction techniques. *Environ. Sci. Technol.* 28, 1698–1705.
- Huber, F., Enzmann, F., Wenka, A., Bouby, M., Dentz, M., Schafer, T., 2012. Natural micro-scale heterogeneity induced solute and nanoparticle retardation in fractured crystalline rock. *J. Contam. Hydrol.* 133, 40–52.
- Huber, F., Seher, H., Kunze, P., Bouby, M., Banik, N.L., Hauser, W., Geckeis, H., Kienzler, B., Schafer, T., 2010. Laboratory Study on Colloid Migration and Colloid-radionuclide Interaction under Grimsel Groundwater Conditions Simulating Glacial Melt-water Intrusion in the Aspo System. KIT INE. Internal Report.
- IAEA, 2001. The Use of Scientific and Technical Results from Underground Research Laboratory Investigations for the Geological Disposal of Radioactive Waste. IAEA, Vienna.
- Ito, K., Kanno, T., 1988. Sorption behavior of carrier-free technetium-95m on minerals, rocks and backfill materials under both oxidizing and reducing conditions. *J. Nucl. Sci. Technol.* 25, 534–539.
- Jaisi, D.P., Dong, H.L., Plymale, A.E., Fredrickson, J.K., Zachara, J.M., Heald, S., Liu, C.X., 2009. Reduction and long-term immobilization of technetium by Fe(II) associated with clay mineral nontronite. *Chem. Geol.* 264, 127–138.
- Jeppu, G.P., Clement, T.P., 2012. A modified Langmuir-Freundlich isotherm model for simulating pH-dependent adsorption effects. *J. Contam. Hydrol.* 129, 46–53.
- Kaplan, D.L., Serne, R.J., 1998. Pertechetate exclusion from sediments. *Radiochim. Acta* 81, 117–124.
- Kienzler, B., Vejmelka, P., Romer, J., Fanghanel, E., Jansson, M., Eriksen, T.E., Wikberg, P., 2003. Swedish-German actinide migration experiment at ASPO hard rock laboratory. *J. Contam. Hydrol.* 61, 219–233.
- Kienzler, B., Vejmelka, P., Romer, J., Schild, D., Jansson, M., 2009. Actinide migration in fractures of granite host rock: laboratory and in situ investigations. *Nucl. Technol.* 165, 223–240.
- Kornfalt, K.A., Persson, P.O., Wikman, H., 1997. Granitoids from the Aspo area, southeastern Sweden - geochemical and geochronological data. *GFF* 119, 109–114.
- Kratz, J.V., Lieser, K.H., 2013. Nuclear and Radiochemistry: Fundamentals and Applications. Wiley.
- Marsac, R., Banik, N.L., Lützenkirchen, J., Buda, R.A., Kratz, J.V., Marquardt, C.M., 2015a. Modeling plutonium sorption to kaolinite: accounting for redox equilibria and the stability of surface species. *Chem. Geol.* 400, 1–10.
- Marsac, R., Banik, N.L., Lützenkirchen, J., Marquardt, C.M., Dardenne, K., Schild, D., Rothe, J., Diascorn, A., Kupcik, T., Schafer, T., Geckeis, H., 2015b. Neptunium redox speciation at the illite surface. *Geochimica et Cosmochimica Acta* 152, 39–51.
- McBeth, J.M., Lloyd, J.R., Law, G.T.W., Livens, F.R., Burke, I.T., Morris, K., 2011. Redox interactions of technetium with iron-bearing minerals. *Mineral. Mag.* 75, 2419–2430.
- McKinley, I.G., Scholtis, A., 1993. A comparison of radionuclide sorption databases used in recent performance assessments. *J. Contam. Hydrol.* 13, 347–363.
- Meyer, R.E., Arnold, W.D., 1991. The electrode potential of the Tc(IV)-Tc(VII) couple. *Radiochim. Acta* 19.
- Meyer, R.E., Arnold, W.D., Case, F.I., Okelley, G.D., 1991. Solubilities of Tc(IV) oxides. *Radiochim. Acta* 55, 11–18.
- Morris, K., Livens, F.R., Charnock, J.M., Burke, I.T., McBeth, J.M., Begg, J.D.C., Boothman, C., Lloyd, J.R., 2008. An X-ray absorption study of the fate of technetium in reduced and reoxidised sediments and mineral phases. *Appl. Geochem.* 23, 603–617.
- Neretnieks, I., 1980. Diffusion in the rock matrix - an important factor in radionuclide retardation. *J. Geophys. Res.* 85, 4379–4397.
- Nockolds, S.R., 1954. Average chemical compositions of some igneous rocks. *Geol. Soc. Am. Bull.* 65, 1007–1032.
- Parkhurst, D.L., Appelo, C.A.J., 1999. User's Guide to PHREEQC (Version 2) - a Computer Program for Speciation, Batch-reaction, One-dimensional Transport, and Inverse Geochemical Calculations, p. 312.
- Peretyazhko, T., Zachara, J.M., Heald, S.M., Jeon, B.H., Kukkadapu, R.K., Liu, C., Moore, D., Resch, C.T., 2008a. Heterogeneous reduction of Tc(VII) by Fe(II) at the solid-water interface. *Geochim. Cosmochim. Acta* 72, 1521–1539.
- Peretyazhko, T., Zachara, J.M., Heald, S.M., Kukkadapu, R.K., Liu, C., Plymale, A.E., Resch, C.T., 2008b. Reduction of Tc(VII) by Fe(II) sorbed on Al (hydr)oxides. *Environ. Sci. Technol.* 42, 5499–5506.
- Rard, J.A., Rand, M.H., Anderregg, G., Wanner, H., 1999. Chemical Thermodynamics of Technetium. Elsevier.
- Ravel, B., Newville, M., 2005. ATHENA, Artemis, Hephaestus: data analysis for X-ray absorption spectroscopy using IFEFFIT. *J. Synchrotron Radiat.* 12, 537–541.
- Rothe, J., Butorin, S., Dardenne, K., Denecke, M.A., Kienzler, B., Loble, M., Metz, V., Seibert, A., Steppert, M., Vitova, T., Walther, C., Geckeis, H., 2012. The INE-Beamline for actinide science at ANKA. *Rev. Sci. Instrum.* 83.
- Schafer, T., Stage, E., Büchner, S., Huber, F., Drake, H., 2012. Characterization of new crystalline material for investigations within CP CROCK. In: 1st Workshop Proceedings of the Collaborative Project „Crystalline Rock Retention Processes“ (7th EC FP CP CROCK), pp. 63–72.
- Schmeide, K., Gürtler, S., Müller, K., Steudtner, R., Joseph, C., Bok, F., Brendler, V., 2014. Interaction of U(VI) with Aspo diorite: a batch and in situ ATR FT-IR sorption study. *Appl. Geochem.* 49, 116–125.
- SKB, 2011. Aspo Hard Rock Laboratory (Annual report).
- Tagami, K., Uchida, S., 1999. Comparison of the TEVA center dot Spec resin and liquid-liquid extraction methods for the separation of technetium in soil samples. *J. Radioanal. Nucl. Chem.* 239, 643–648.
- Um, W., Serne, R.J., 2005. Sorption and transport behavior of radionuclides in the proposed low-level radioactive waste disposal facility at the Hanford site, Washington. *Radiochim. Acta* 93, 57–63.
- USEPA, 1999. The Kd Model, Methods of Measurement, and Application of Chemical Reaction Codes, Understanding Variation in Partition Coefficient, Kd Values. United States Environmental Protection Agency, Office of Air and Radiation, p. 212.
- Videnska, K., Havlova, V., 2012. Retention of Anionic Species on Granite: Influence of Granite Composition. *Waste Management* 2012. Phoenix, Arizona, USA.
- Viollier, E., Inglett, P.W., Hunter, K., Roychoudhury, A.N., Van Cappellen, P., 2000. The ferrozine method revisited: Fe(II)/Fe(III) determination in natural waters. *Appl. Geochem.* 15, 785–790.
- Wester, D.W., White, D.H., Miller, F.W., Dean, R.T., Schreifels, J.A., Hunt, J.E., 1987. Synthesis and characterization of technetium complexes with phosphorus-containing ligands - the homoleptic trimethylphosphite, dimethylmethylphosphonite and methyl-diethylphosphinito technetium(I) cations. *Inorg. Chim. Acta* 131, 163–169.
- Westsik Jr., J.H., Cantrell, K.J., Serne, R.J., Qafoku, N.P., 2014. Technetium Immobilization Forms (Literature Survey), PNNL-23329.
- Wildung, R.E., Li, S.W., Murray, C.J., Krupka, K.M., Xie, Y., Hess, N.J., Roden, E.E., 2004. Technetium reduction in sediments of a shallow aquifer exhibiting dissimilatory iron reduction potential. *Fems Microbiol. Ecol.* 49, 151–162.
- Xu, S., Worman, A., 1999. Implications of sorption kinetics to radionuclide migration in fractured rock. *Water Resour. Res.* 35, 3429–3440.
- Zachara, J.M., Heald, S.M., Jeon, B.-H., Kukkadapu, R.K., Liu, C., McKinley, J.P., Dohnalkova, A.C., Moore, D.A., 2007. Reduction of pertechetate [Tc(VII)] by aqueous Fe(II) and the nature of solid phase redox products. *Geochim. Cosmochim. Acta* 71, 2137–2157.

Repository KITopen

Dies ist ein Postprint/begutachtetes Manuskript.

Empfohlene Zitierung:

Huber, F. M.; Totskiy, Y.; Marsac, R.; Schild, D.; Pidchenko, I.; Vitova, T.; Kalmykov, S.; Geckeis, H.; Schäfer, T.

[Tc interaction with crystalline rock from Äspö \(Sweden\): Effect of in-situ rock redox capacity](#)
2017. Applied geochemistry, 80, 90–101.
[doi:10.5445/IR/1000068977](https://doi.org/10.5445/IR/1000068977)

Zitierung der Originalveröffentlichung:

Huber, F. M.; Totskiy, Y.; Marsac, R.; Schild, D.; Pidchenko, I.; Vitova, T.; Kalmykov, S.; Geckeis, H.; Schäfer, T.

[Tc interaction with crystalline rock from Äspö \(Sweden\): Effect of in-situ rock redox capacity](#)
2017. Applied geochemistry, 80, 90–101.
[doi:10.1016/j.apgeochem.2017.01.026](https://doi.org/10.1016/j.apgeochem.2017.01.026)

Lizenzinformationen: [CC BY-NC-ND 4.0](#)